RESPONSE OF ENTRAINED AIR-VOID SYSTEMS IN CEMENT PASTE TO PRESSURE

By

ROBERT FRAZIER

Bachelor of Science in CIVIL ENGINEERING

Oklahoma State University

Stillwater, OK

2008

Submitted to the Faculty of the
Graduate College of the
Oklahoma State University
in partial fulfillment of
the requirements for
the Degree of
MASTER OF SCIENCE
July, 2011

RESPONSE OF ENTRAINEDAIR-VOID SYSTEMS IN

CEMENT PASTE TO PRESSURE

Thesis Approved:

Dr. Tyler Ley

Thesis Adviser

Dr. Bruce Russell

Dr. Steve Cross

Dr. Rifat Bulut

Dr. Mark E. Payton

Dean of the Graduate College

TABLE OF CONTENTS

LIST OF TABLES

Table Page

LIST OF FIGURES

Figure Page

CHAPTER I

INTRODUCTION

This research was initiated in an attempt to understand the behavioral mechanisms which control the response of an entrained air-void system under pressure, specifically under pressures typically seen during an ASTM C231 Type B pressure meter test. Where other research has hypothesized on these mechanisms to explain discrepancies between pressure meter results and hardened air-void analysis, this research utilizes micro-computed tomography to visualize the response of the air-void system in fresh cement paste. The primary objectives were to measure compression of individual air-voids, and to quantify the number and volume of air-voids lost to dissolution into free water. The purpose of these objectives is to check the accuracy of the Type B pressure meter.

CHAPTER II

RESPONSE OF ENTRAINED AIR-VOID SYSTEMS IN CEMENT PASTE TO PRESSURE

As the most commonly employed construction material in the world, concrete has been researched extensively for methods to increase the service life. Wherever concrete can become saturated and freezing temperatures occur, damage can occur within the hardened concrete.

To promote frost durability in these mixtures air-entraining agents (AEA's) are used to develop and stabilize an air void system during mixing. AEA's are essentially surfactants that repel negatively charged cement particiles, and thus create air voids of specific sizes within the fresh concrete paste. These entrained voids are typically between 10 μm and 1 mm and are essential to prevent freeze thaw damage.[1-4]

A number of studies demonstrate that the size and distribution of these air-voids are the most important parameters to determine the frost durability of concrete.[2] However, because it is not currently possible to reliably measure the distribution of these voids in fresh concrete, specifications instead require a specified volume of air in the concrete. This volume measurement can be misleading though because it does not consider size and distribution of the air-voids. Thus it is possible that although the volume requirements were met, the actual grading and distribution of the air-void system does not protect a sufficient amount of paste in the

concrete. Currently, the most widely used method to measure the air-void system in fresh concrete is the type B ASTM C 231 pressure method.

Previous researchers have documented discrepancies between pressure meter air measurements and methods such as microscopic analysis, and have attempted to provide a range of explanations for such differences.

This research aims to improve our understanding regarding the performance of an ASTM C231 pressure meter and determine the situations when this meter may not be accurate. In particular, the following will be discussed: (1) verify the accuracy of Boyle's Law to predict air-entrained bubble response to over pressure, and (2) quantify the dissolution of smaller voids from applied overburden pressures.

Background

History of the ASTM C 231 Type B Pressure Meter

In 1946, Klein and Walker published an article detailing the concept of a device which calculated the air content in a concrete mixture by measuring the deformation of a known volume of the concrete when an overburden pressure was applied.[5] This device assumes that air trapped during mixing is the only phase in the mixture that is compressible. Other materials in the sample, such as aggregate and water, are considered incompressible at the range of pressures used for this test. The pressure meter model also assumes that the response of air-voids to overpressure can be explained by Boyle's Law. A correction procedure has been applied in the ASTM method to account for the air contained by the aggregates.

A modern ASTM C 231 Type B pressure meter essentially has two chambers. The lower chamber contains a quarter cubic foot of concrete that is consolidated and leveled in a standard manner along with some added water to completely fill the chamber. The other chamber holds a

known volume of pressurized air that is used to load the bottom chamber. A lever is used to release the pressurized air into the lower chamber. The lower chamber will respond to this air by decreasing in volume from the pressure. Boyle's Law is used to estimate the amount of air that was in the concrete based on the resultant equilibrium pressure between these two chambers. Figure1 gives an overview of this process showing a single void in the mixture.

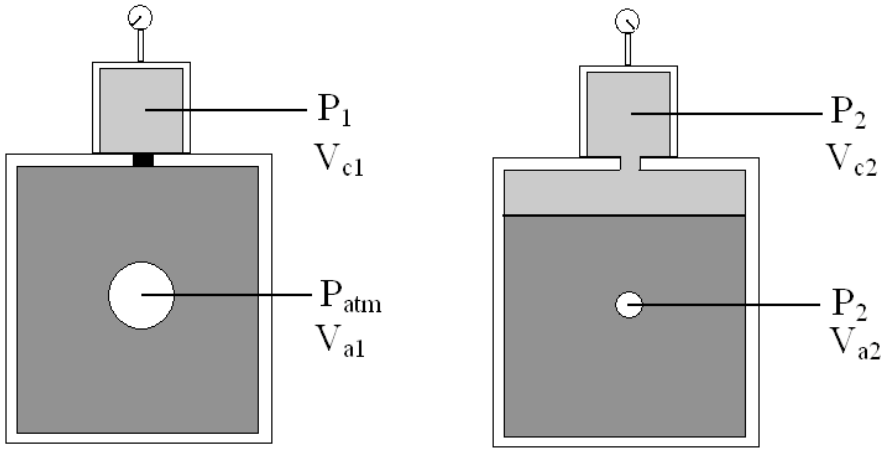

Figure 1: Initial and Equilibrium States of the Type B Pressure Meter (After Hover[6])

The two major equations used by the type B pressure meter to determine the volume of air in a concrete sample are shown in Eq. 1 and 2. These equations were adapted from those shown by Hover[6]. Equation 1 shows that the equilibrium pressure is a function of the change in volume of the air-void system. Equation 2 uses this equilibrium pressure to determine the atmospheric volume of air in the concrete. The second equation uses Boyle's Law to relate the equilibrium pressure to the original volume of air in the concrete. Figure 3 shows the result of these equations when input with known values for P1, Patm and Vc1. In reality, P2 is a direct measurement from the pressure gauge in the upper chamber of the pressure meter and then this pressure is used with Eq. 2 to determine the volume of air in the sample chamber. For the example shown in Figure 2, the initial pressure in the upper chamber was 1 atm above atmospheric pressure, and the volume of the upper chamber was taken to be 480.1 cm^3.

$$P_2 = P_1 V_{c1}/(V_{c1}+\Delta V_a) \quad \text{Eq. (1)}$$

$$V_{a1}=V_{c1}((P_1-P_2)/(P_2-P_{atm})) \quad \text{Eq. (2)}$$

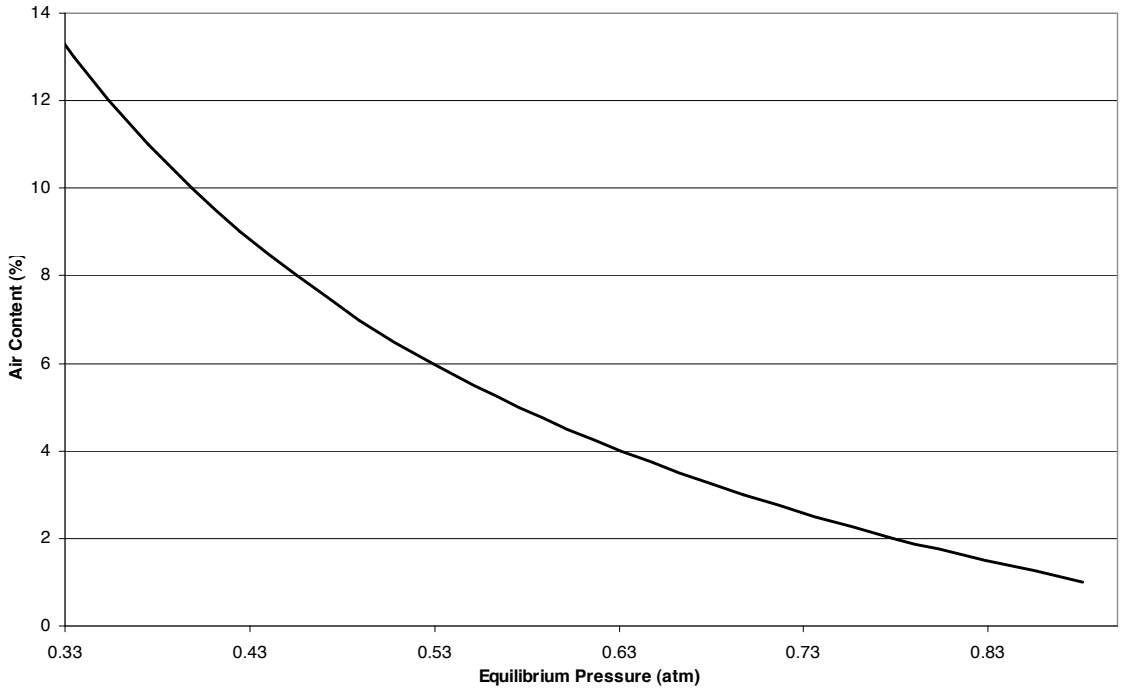

Figure 2: Equilibrium Pressure – Air Content Calibration for Pressure Meter

There have been numerous publications discussing discrepancies between ASTM C231 pressure meter readings and ASTM C457 microscope analysis, a procedure which measures and counts air-void chord lengths at a given polished cross section of a hardened concrete sample. Gay has demonstrated that these discrepancies exist under certain conditions, such as elevated mixing and placement temperatures[7,8] , high air contents[7], or due to a high percentage of small voids in the system.[9] Gay first reported that entrained air-void systems with a large percent of small air-voids, such as that created by synthetic air-entraining agents (AEAs), may have inaccurate readings from the pressure meter.

Other researchers have reported comparisons between the two methods, but these reports are not in agreement. Some have found the pressure meter to register lower air contents than the

microscopic analysis,[10] while others have shown it to register higher contents.[11] There are also reports that variance is statistically insignificant.[12]

It has been hypothesized that discrepancies in pressure meter readings are due to the relative incompressibility of small voids.[6,9] An assumption was made during the derivation of pressure meter calculations that the internal air pressure in a void is equal to atmospheric pressure. The actual internal pressure of a void is shown in Equation (3), where Pi is the internal pressure, Po is the external pressure, R is the bubble radius and τ is the surface tension of the void surface.[13] This equation shows that as voids become smaller, their internal pressure increases. By ignoring the second term of Equation (3), all voids are assumed to have the same internal pressure. Hover performed theoretical work to demonstrate the affect of this assumption. This work examined the errors associated with varying surface tension values. The work showed that for bubble walls with surface tensions less than or equal to that of water the errors associated are insignificant.

$$P_i=P_o+2T/R \qquad \text{Eq. (3)}$$

Previous research has also shown that when a void system is subjected to pressure, small air-voids will dissolve into the free water.[13] This is due in part to Henry's Law which states that the concentration of dissolved gas in a solution is proportional to the partial pressure of the gas out of solution. When an overburden pressure is applied it can be shown in equation 6 that the smallest air-voids will have the highest internal pressure. When this pressure becomes high enough the gas in the void will enter the surrounding liquid and the void will collapse. The research performed on this topic investigated the changes in void-size distribution when subjected to pressures upwards of 1050 kPa, then returned to atmospheric pressure. Although this was useful for demonstrating the affect of pumping on concrete and displaying the changes which occurred, the research failed to investigate this behavior for small pressures such as those seen during the use of the ASTM C231 pressure meter.

Micro-Computed Tomography

One challenge with previous research on this topic is that it is very difficult to directly observe the changes of the void systems in the cement paste from these external pressures. An attempt was made to address this problem in this research by using a Skyscan 1172 micro-CT scanner. In the remainder of the document it will be known as mCT. This piece of equipment allowed 3D images to be captured of the internal structure of materials. This allowed direct observations to be made of the void systems in fresh paste. This unit has the ability to image details down to 1 μm in size. This allowed voids that are approximately 5 μm in diameter to be imaged. A brief overview of computed tomography is provided below. Additional information concerning this technology may be found in the references.[14-16]

The micro-CT produces a number of radiographs of a sample that are taken at very small angular rotations. These radiographs are generated by aligning a sample between an x-ray source and an x-ray detector. The x-rays which pass through the sample are captured by the detector, leaving an image of the internal structure of the sample. These radiographs are combined to create a series of 2D slices from the sample and these 2D slices can be combined to create a 3D image. A schematic of this process is shown in Figure 3. A typical radiograph and reconstructed cross section are shown in Figure 4 with air-voids appearing as black circles in the cross section on the right. The remaining material is paste.

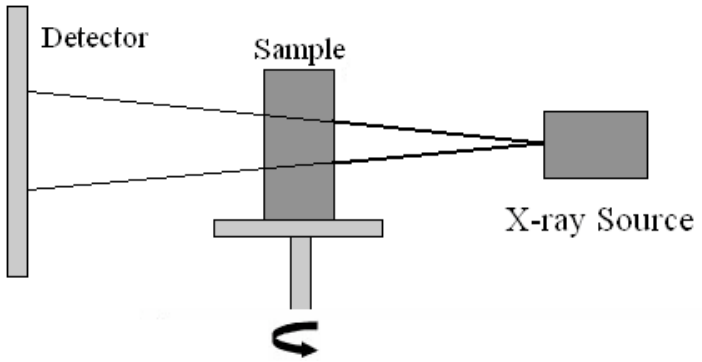

Figure 3: Schematic of 1172 radiograph process

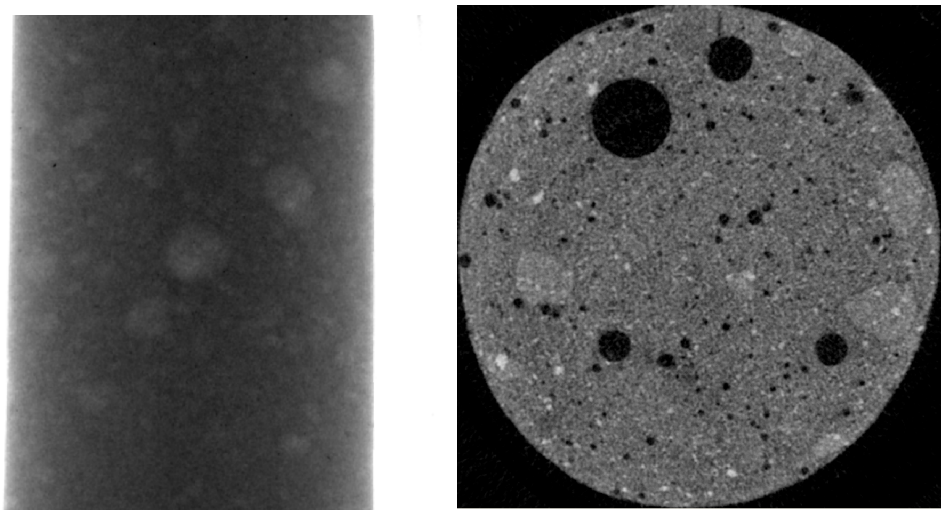

Figure 4: Typical radiograph – Cylindrical Paste Sample – 5mm Diameter

Procedural Overview

Using a micro-CT scanner, concrete paste samples were studied for the affects of overburden pressures on the air-entrained void systems. These experiments allow direct observation of how air-void systems change in fresh cement paste from these pressures and will assist in answering questions about the effectiveness of a pressure meter to measure the air-void system in concrete.

Two types of experiments were conducted. The first consisted of scanning cement paste samples to quantify the response of individual air-voids larger than 50 microns to these pressures. The second used the microCT to measure the response of the entire air-void system to these pressures.

The general process for each experiment began by preparing a paste mixture according to ASTM C305, taking a unit weight measurement of the mixture according to ASTM C311, then preparing a sample to be scanned with the mCT. This took approximately ten minutes to complete from the time cement initially touched water. After this, the mCT was setup for the particular parameters used for these scans. The atmospheric pressure scan was completed first and took approximately 30 minutes. This is a typical time taken for all subsequent scans. The sample was then pressurized to a predetermined value by using an external pneumatic system and then scanned again. Temperature readings were taken from the sample prior to scanning and after each subsequent scan with an infrared thermometer to check the change in temperature induced by exposure to x-rays. This was process was repeated for each pressure step. For the first phase of experiments, scanning was completed in 110 minutes; for the second, the experiment was completed in 170 minutes.

Each scan resulted in a set of radiographs which were reconstructed into cross-sectional images through the sample. For each set of images, the air system was isolated from the concrete paste. Next, geometric data for individual air-voids was calculated, such as volume, surface area, and centroids within the sample. All processing and data was generated with Skyscan CTAnalyzer Version 1.8.1.2.

Materials

Raw materials consisted of Portland cement (ASTM C 150 Type I), tap water, wood rosin, synthetic, and Vinsol resin AEAs.

Additionally, a hydration stabilizer based on hydroxycarboxylic acid salts and compound carbohydrates which conformed to ASTM standards was used in mixes for the 170 minute experiments to delay hydration of the paste. This was necessary because samples that had been hydrating for over two hours were observed to no longer respond to pressurization. The dosage used was approximately 1.8 grams of hydration stabilizer per kilogram of cement. This dose was determined to be sufficient for delaying set time of the paste sample without affecting the stability of the air-void system by scanning a mixture at atmospheric pressure every thirty minutes and no difference was observed in the void system.

All mixtures were prepared to guidelines specified in ASTM C305. As specified, ingredients including AEA's and hydration stabilizer, if required, were added during the first minute of mixing. Table 1 below summarizes the mix design for each experiment. All mixtures had a water to cement ratio of 0.42. A constant volume was achieved with a cement content of 1373 grams and a water content of 576.8 grams of water. The air content was determined from a unit weight measurement as specified in ASTM C138.

Table 1: Concrete Paste Mixture Design

Phase	AEA	Air Content (ASTM C138)
1	wood rosin	6%
	synthetic	5.5%
	Vinsol resin	6.5 %
2	wood rosin	5.5%
	wood rosin	12%
	synthetic	5.5%
	Vinsol resin	6.5 %

Sample Preparation

Samples were made by filling a capillary tube up to a height of three millimeters with cement paste. The capillary tubes had a diameter of 0.5 cm and were made of a polypropylene plastic. These dimensions were fixed by the pixel area of the detector (2000 x 1048) as well as the pixel size (4.9 um/pixel). Although it is not necessary for the entire sample to fit within the scanning window, it was decided that a smaller sample which could fit was best for these experiments. This was chosen so that the meniscus bowl at the top of the sample could be used to provide useful data about the global volume change of the sample and provide a double check to the observed void changes Hmmmm.

In order to minimize disturbance of the air-void system, the bottom three millimeters of the tube was placed in the mixture and allowed to fill. Capillary forces kept the paste in the tube until clay putty could be placed in the bottom of the tube. Next, two millimeters of water was placed on top of the paste. The water was used to prevent plastic shrinkage cracks during the scanning process. A photo of a typical sample is shown in Figure 6 below. Also need a call-out in the text for Fig. 5.

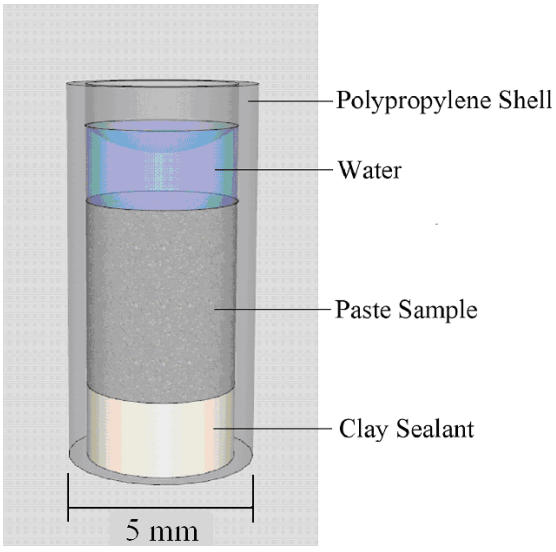

Figure 5: Typical Paste Sample

Experimental Equipment

Ideally, one would be able to leave a pressure source connected to the vessel throughout the scan to ensure a maintained pressure. However, it was not possible to do this in the testing chamber. Therefore all tests were run in a stand-alone vessel.

A pressure vessel was constructed that met the spatial limitations of the Skyscan 1172 chamber but had minimal x-ray absorbance to prevent interference with sample absorption. The final pressure vessel was constructed of a methyl methacrylate tube with a female threaded copper collar. The lid of the vessel is a one-way pressure valve with male threads to match the copper collar of the vessel. The diameter of the vessel was 12.5 mm and measured 40 mm tall. A picture of the pressure vessel is shown in Figure 6.

Figure 6: Final Pressure Vessel

During the testing, the paste sample was placed in the stand alone pressure vessel. Scans were taken at atmospheric pressure as a baseline for the testing and then removed from the Microphotonics 1172. The pneumatic system was then used to increase the pressure in the vessel. During the pressurization process, the vessel was gently tapped on the table top. This was done because of the thixotropic nature of the paste. The vibration causes the plastic yield stress of the paste to be exceeded and the material to act like a liquid and respond to the pressure{OK good

explanation}. This tapping provides the same result as the rapping of a mallet against the concrete container during an ASTM C231 pressure meter test.

The valve used in the pressure vessel had a spring-loaded closing mechanism so that minimal pressure loss occurred when disconnecting the vessel from a pressure source. In order to account for this loss, a calibration experiment was conducted to quantify the pressure difference when the valve was disconnected. This was done by replacing the body of the vessel with a pressure gauge. The pressure loss was then measured as the system was pressurized and then removed. For example the valve/gauge assembly was pressurized to 1 atm according to the gauge at the pressure source. The valve was then disconnected and the resultant pressure inside the assembly was 0.983 atm, creating a volume loss equal to 0.017 atm. This was done ten times for the range of pressures used in the paste experiments. The standard deviation for the loss at each pressure step was around 0.005 atm. This allowed a correction factor to be determined for the test setup that allowed a repeatable pressure to be achieved in the pressure vessel.

Pressurization of the sample was conducted with a pneumatic system constructed of a compressor in line with a pressure gauge and a variable-opening relief valve. The relief valve was in between the compressor and gauge and was hand-controlled to attain different pressures. This setup is shown in Figure 7.

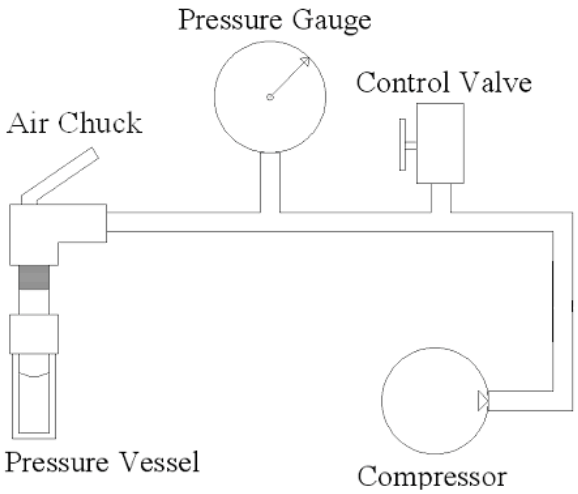

Figure 7: Pneumatic System Configuration

The parameters used for the settings of the Skyscan 1172 are summarized in Table 2. The detector area was chosen in order to obtain a voxel size that was small enough to provide useful details and a scan time that was not excessive. A higher resolution scan was possible, but the constraints of set time made this unfeasible. A high hydration stabilizer dosage could have been used but this would have exceeded the manufacturers recommended dose. Additionally, lower resolution scans could have been attempted that require a lower amount of exposure time to obtain a satisfactory image. This would have eliminated the need for a stabilizer in the second phase of experiments, but there was a concern that this would hinder imaging of air-voids in the size range below 50 microns. This size range is the most abundant in number in most entrained air-void systems. The parameters listed in Table 2 were decided upon as the best balance between scan time and imaging capabilities.

The next major parameter determined was the filter. Filters are thin metal sheets which remove certain ranges of the x-ray wavelength spectrum, depending on the metal used. Previous scans have shown that by using no filter, beam hardening artifacts become a concern. Beam hardening is an artifact which results from the outside of a sample absorbing low energy x-rays. This causes

the outside of the sample to look brighter/denser than similar material at the core of the sample. It was the goal of the research team to find scan parameters that uses a minimal amount of image correction. An aluminum filter provided a high signal to noise ratio for the gas phase inside of the air-voids, which allowed for increased accuracy when isolating air-voids from the rest of the paste. Once the filter choice was made, a voltage was chosen. Although there is a range of voltages which may have provided a sufficient signal to noise ratio, one value was selected to standardize all scans conducted. This voltage, as with the filter selection, provided a signal to noise ratio which minimized the amount of noise present in the gas phase of the sample. This was done to simplify the process of identifying the air-voids. The Skyscan 1172 has a fixed relationship between voltage, current and power so the remaining parameters were fixed.

Table 2: Summary of Skyscan 1172 Scan Parameters

Parameter	**Value**
Detector Area	2000 x 1048
Pixel Size	4.9 um/pixel
Voltage	100 kV
Current	100 uA
Power	10 W
Filter	0.5 mm Aluminum
Frame Averaging	3 frames
Rotation Step	0.3 degrees

Next algorithms are used to transform a series of radiographs into a series of 2D slices and then a 3D model. During the reconstruction it is also common to post process the data to remove artifacts. Typically artifacts corrected include beam hardening, ring artifacts, and misalignment

artifacts. More information on artifact origins and correction algorithms is referenced[16]. The software, Skyscan NRecon V 1.6.2.0, was used for all reconstruction work. This software contains correction algorithms for each artifact with one controllable parameter per artifact. This single parameter will be addressed as the correction factor henceforth.

To determine the amount of correction needed, a preview slice was created from the scan with no artifact correction. Next artifact corrections were applied to this preview slice. The corrections were increased until the artifacts were not visible. Work was also done to check the regularity of the gray scale in the preview slice. The primary correction needed was for ring artifacts. No misalignment artifacts were observed and the beam hardening was minimized by the filter.

Once the data sets had been created they were processed with Skyscan CTAn 1.8.1.2 in order to make measurements of the air-void size and location. To do this the images were segmented with a histogram-based thresholding technique so that the air-voids were differentiated when compared to the rest of the sample. Other segmentation techniques, such as boundary detection and smoothing-based methods, were considered; however due to the importance placed on detecting voids only a few voxels large, a histogram based method was used to ensure that no information was lost about these voids. With other methods, small features such as the smallest voids are overlooked or removed to present a clean representation of the larger features. The histogram method allows the user to segment an image into black and white groupings without any manipulation of the image itself, ensuring that no information is lost on small features.

The process of grouping grayscale ranges into phases is known as thresholding. With histogram-based thresholding techniques one chooses a certain gray scale number and everything above that line is considered black and everything below is white. It was not possible to use this technique directly because of noise observed inside of the air-voids. This noise created a distinct overlap between the air phase and paste phase in grayscale frequency plots. This is shown in Figure 8.

These figures were generated by summing the grayscale values present in 20 different paste regions and 20 air-voids that were chosen by inspection. This graph shows that in order to capture all of the air within a sample then a thresholding range of 0-40 would be needed, and to capture all cement paste a range of 10-120 would be needed. The grayscale range from 10 to 40 thus applies to both phases. To use a threshold range of 0-10 for air-voids would mean roughly 10% of the volume of air-voids was not captured. To use a range from 0-40 would mean that 5% of the paste would be counted as air-voids.

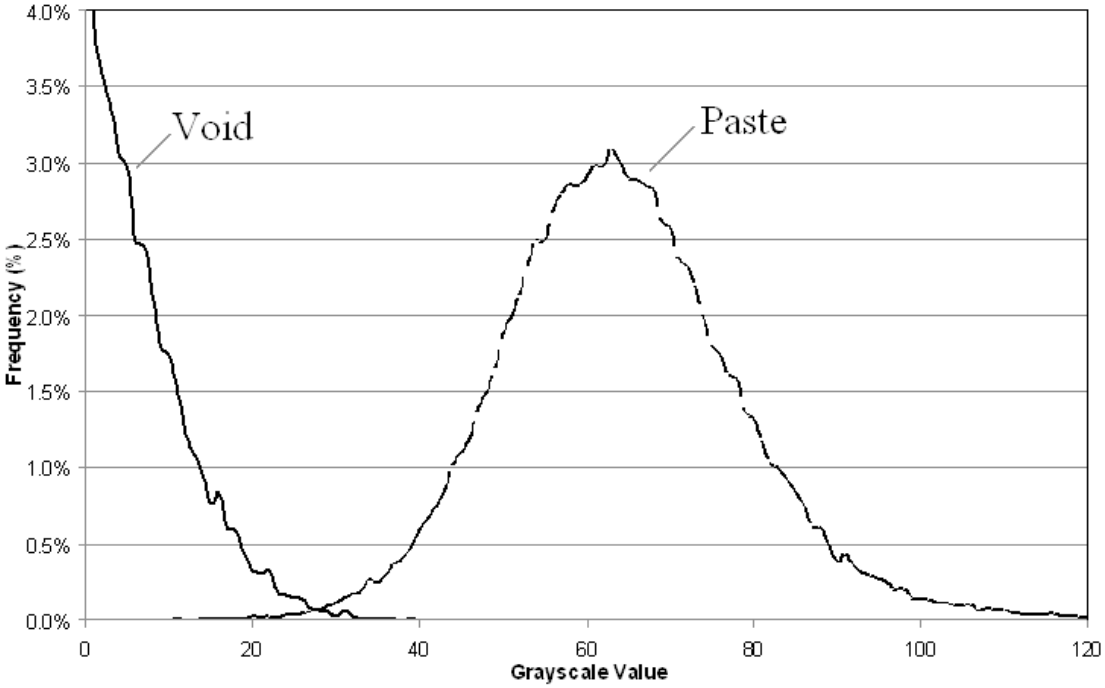

Figure 8 – Plot of frequency versus grayscale for 20 different points in the paste and in a void

To address this issue it was decided to use a threshold value of 20 so that minimal paste was included in the air-void thresholding. This resulted in a thresholded image similar to what is shown in Fig. 9 (b). Next a despeckle routine was used. This routine eliminated black voxel configurations with a volume less than 1000 cubic voxels. This ensured collection of black voxels that was completely surrounded by white voxels would be removed. If any part of the black voxels connected with the black pixels identified as paste then it was not removed. This image

processing technique allowed the noise in these voids to be removed and hence an improved estimate of the voids volume. Figure 9 (c) demonstrates the affect of this despeckle routine. One challenge with using this histogram based thresholding technique is there will be some errors when the technique estimates the boundary of the void. This occurs because the gray scale intensity of a voxel is an average of all of the material in that volume. If this voxel represents a volume that is partially full of air and paste then the gray scale value would be a weighted average of these two materials. While it is challenging to quantify this error it should not be significant as it may only impact a few voxels.

With the techniques presented so far it was possible to remove noise which appears within air-voids. However, noise within the paste still exists. This noise appears falsely as only a few single voxels. These individual voxels must also be removed so that they are not assumed to be small air-voids. With the resolution used for these experiments, it is difficult to distinguish this noise from actual voids. To address this it was decided to remove all objects which could possibly be noise. This resulted in a minimum void to be considered. This minimum air-void size was chosen as 7 voxels as this was seen as the largest noise object. This minimum void is shown in Fig. 10. This leads to an air-void of diameter of 20 μm to be considered the smallest air-void possible in the analysis. This step of despeckling removed white objects less than seven voxels in size is shown in Figure 9 (d). Figure 11 provides a sample 3D model generated after the processing steps of Figure 9 were performed. It shows a section of a paste sample at varying transparency levels.

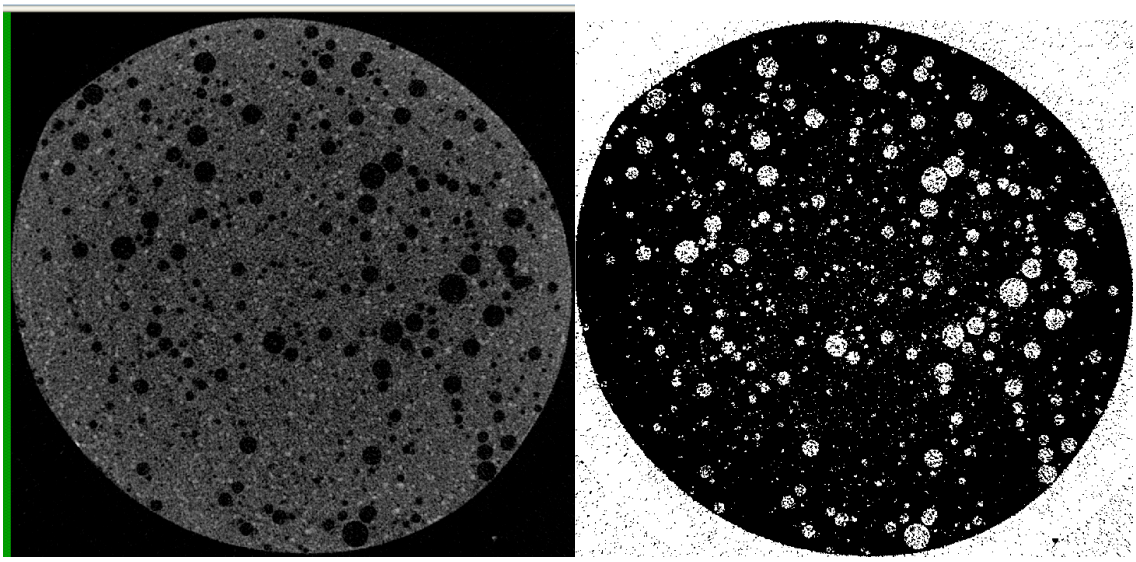

(a) Original Reconstructed CT Slice (b) CT Slice with Binary Threshold Applied

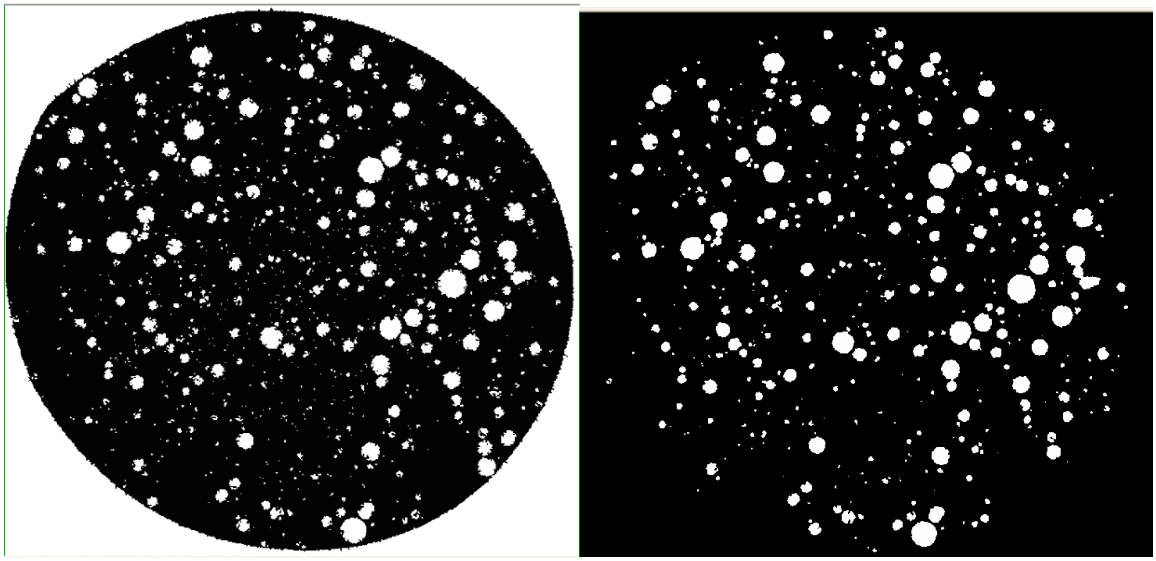

(c) Despeck Black less than 1000 Voxels (d) Despeck White less than 7 Voxels

Figure 9: CT Image, Reduced Air Threshold, Despeckle

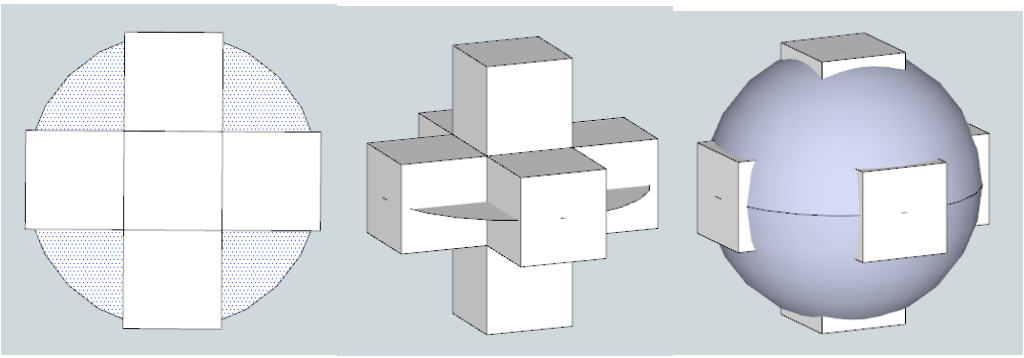

Figure 10: Minimum Air-void Size Representation

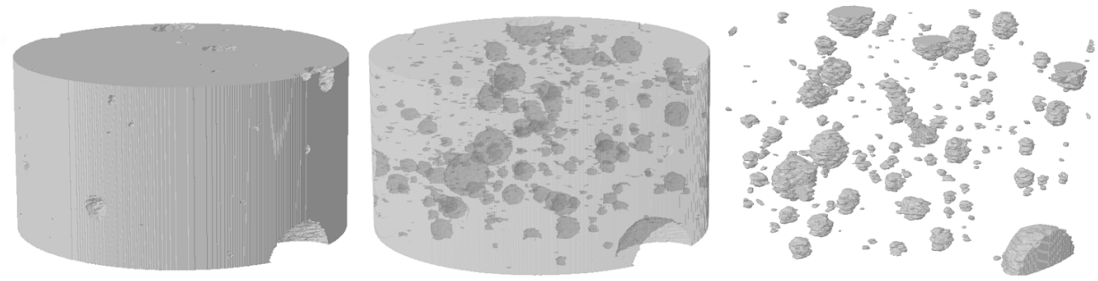

Figure 11: 3D Model of Processed Air-void System

In addition to the above mentioned steps for image processing, a step was included to remove all objects which touched a border of the sample. Any air-void in contact with a border of the sample was removed to prevent an incomplete volume being returned numerically and thus causing errors when comparing to the performance of voids in future pressure steps. In addition the air outside of the paste sample was removed. This was necessary to ensure accurate gross measurements of air content in the sample.

Skyscan CTAnalyzier 1.8.1.2, a processing program, was used to assemble any remaining white voxels into 3D objects. It was then possible to determine a volume and centroid for the air-voids in the sample. These volumes were then used to calculate diameters of the bubbles assuming a spherical shape for each object.

Methodology

Response of Air-void Size to Pressure

For this phase, the objective was to determine how entrained air-voids compress under overburden pressure. Currently, the ASTM C 231 pressure meter assumes that all air-voids follow Boyle's Law when they are pressurized.[5] Because the equilibrium pressure of a pressure meter is around 0.5 atm for most air-entrained concretes that contain 6% air, this pressure was chosen as an important pressure step in determining the samples response to pressure. To investigate response of air-voids in the operable range of the pressure meter, air-entrained samples were scanned at atmospheric pressure, 0.5 atm, and 1 atm. The atmospheric pressure scan was used to have a baseline image to compare subsequent pressurized scans.

For these experiments, individual air-voids were tracked across each pressure step and the volume change. In order to track an air-void, a routine was developed which used the centroids and diameters for each air-void at atmospheric pressure and to find its location and diameter in the next pressure step. This data was presented as a diameter change ratio to ease comparison to Boyle's Law predictions. Table 3 below displays the theoretical changes in volume and diameter a void would experience for each pressure step according to Boyle's Law. These values represent the theoretical compression ratios that all voids were compared against. These are the same values used by the pressure meter when assuming that internal pressure of the voids is equal to the external pressure.

Table 3: Theoretical Values for Boyle's Law Compression of Individual Air-voids

	Boyle's Law Values	
Pressure (atm)	Volume Ratio (V_2/V_1)	Diameter Ratio (D_2/D_1)
0.33	0.746	0.907
0.5	0.667	0.872
0.67	0.595	0.841
1	0.495	0.791
1.33	0.424	0.751

The smallest atmospheric air-void considered for tracking was one with a 50 micron diameter. This was due to the difficulty in tracking individual voids below this point. Voids below this size are so numerous that the tracking routine, which operates on identifying similar centroids, identifies multiple objects as possible matches to every atmospheric void. Additionally, voids below this size were discovered to dissolve, making matches impossible.

Dissolution of Air-Voids Under Pressure

The second phase of experiments was designed to better understand the dissolution of air-voids from increasing fluid pressure. As mentioned previously, small air-voids have higher internal pressures than larger voids, making them more likely to dissolve when exposed to overburden pressures as predicted by Henry's Law. The intent of this phase was to measure the entire void system at each pressure step, and by comparing the measurements to predictions made by Boyle's Law, determine the number and size of voids which dissolved. For these experiments, scans were done at atmospheric, 0.33, 0.67, 1 and 1.33 atm. The sample preparation and scan parameters were the same as was previously used with the addition of a hydration control admixture to control mixture stiffening.

In these tests it was not possible to follow individual bubbles during the pressurization steps because of the large number of small bubbles in the samples and the eventual dissolution of these bubbles. Instead the size distribution of the air-void system was measured at different pressure steps. A comparison could be made between the actual air-void distribution and that predicted by Boyle's Law. Analysis was concentrated on determining the variance of measured volume to that predicted by Boyle's Law at each pressure step, then studying differences in the air-void system at different pressure steps to pinpoint which air-void sizes were responsible for creating this difference.

Data was also generated for the total volume measured at each pressure step. These measured volumes, as with air-void size distributions, were compared against volumes suggested by Boyle's Law. Because these theoretical values do not consider the loss of volume to dissolved air-voids, the difference between measured volume and theoretical volume is assumed to be a function of the volume of air-voids dissolved.

For each pressure step an air-void size distribution curve was generated which displayed the quantity of air-voids measured in 5 micron diameter increments. The atmospheric air-void system was also used to generate theoretical size distribution curves for each pressure step if only Boyle's law compression occurred. This was done by applying the compression ratios shown in Table 3 to each void, then sorting them into size groups.

To summarize, air-void size distribution curves were generated from each scan. Additionally, theoretical curves were generated which show how the void size distribution would change only if Boyle's Law compression occurred. The primary purpose of this curve type was to determine which size range of air-voids were predominantly going in to solution by comparing predicted Boyle's Law curves to the measured system.

Results

Response of Air-void Size to Pressure

Given below are the results of the Boyle's Law experiments conducted for each air entrainer. Table 4 provides the statistical data gathered during the experiments which monitored the compression of individual air-voids. Air-voids were broken into size ranges in an attempt to measure compression of different ranges independently.

Each pressure step lists the number of voids tracked, the average diameter change expressed as a ratio of the original diameter, the standard deviation, and the percent of air-voids within one

standard deviation. The percent of air-voids within one standard deviation of the average was used to compare the data points distribution against percentages seen in a normally-distributed data population.

Table 4: Air-Void Compression Results

	0.5 atm					1 atm				
Size at Atm. Pressure (μm)	Number Investigated	Avg (D_2/D_1)	σ	CV	% Diff. from Theoretical	Number Investigated	Avg (D_2/D_1)	σ	CV	% Diff. from Theoretical
Wood Rosin										
49-73	2394	0.881	0.066	7.49%	1.26%	1317	0.814	0.066	8.11%	3.04%
74-98	1442	0.838	0.069	8.23%	3.68%	1343	0.76	0.055	7.24%	3.80%
98-147	845	0.832	0.052	6.25%	4.37%	781	0.754	0.062	8.22%	4.56%
> 147	330	0.83	0.049	5.90%	4.60%	274	0.755	0.05	6.62%	4.43%
Total	5011	0.854	0.067	7.85%	1.84%	3715	0.777	0.066	8.49%	1.65%
Synthetic										
49-73	1037	0.887	0.056	6.31%	1.95%	414	0.812	0.065	8.00%	2.78%
74-98	1674	0.876	0.054	6.16%	0.69%	981	0.786	0.064	8.14%	0.51%
98-147	987	0.865	0.051	5.90%	0.57%	866	0.765	0.055	7.19%	3.16%
> 147	291	0.868	0.051	5.88%	0.23%	263	0.755	0.059	7.81%	4.43%
Total	3989	0.875	0.054	6.17%	0.57%	2524	0.78	0.064	8.21%	1.27%
Vinsol Resin										
49-73	1085	0.871	0.063	7.23%	0.11%	611	0.813	0.067	8.24%	2.91%
74-98	1913	0.854	0.063	7.38%	1.84%	768	0.764	0.056	7.33%	3.29%
98-147	1260	0.83	0.059	7.11%	4.60%	494	0.75	0.063	8.40%	5.06%
> 147	375	0.827	0.05	6.05%	4.94%	232	0.732	0.052	7.10%	7.34%
Total	4633	0.85	0.063	7.41%	2.30%	2105	0.772	0.067	8.68%	2.28%
Theoretical		**0.87**					**0.79**			

Dissolution of Air-Voids Under Pressure

The results for this testing are summarized in Figure 12. This figure shows how the volume of air changes with increasing pressure when compared to the values predicted by Boyle's Law ($V_2/V_1 = P_1/P_2$). All volume values have been normalized to allow comparison of the samples. The vertical line represents the equilibrium pressure in a pressure meter which corresponds to 6% and 3% air. Additionally, Figure 13 provides the air-void size distribution curve measured for each air entrainer at atmospheric pressure.

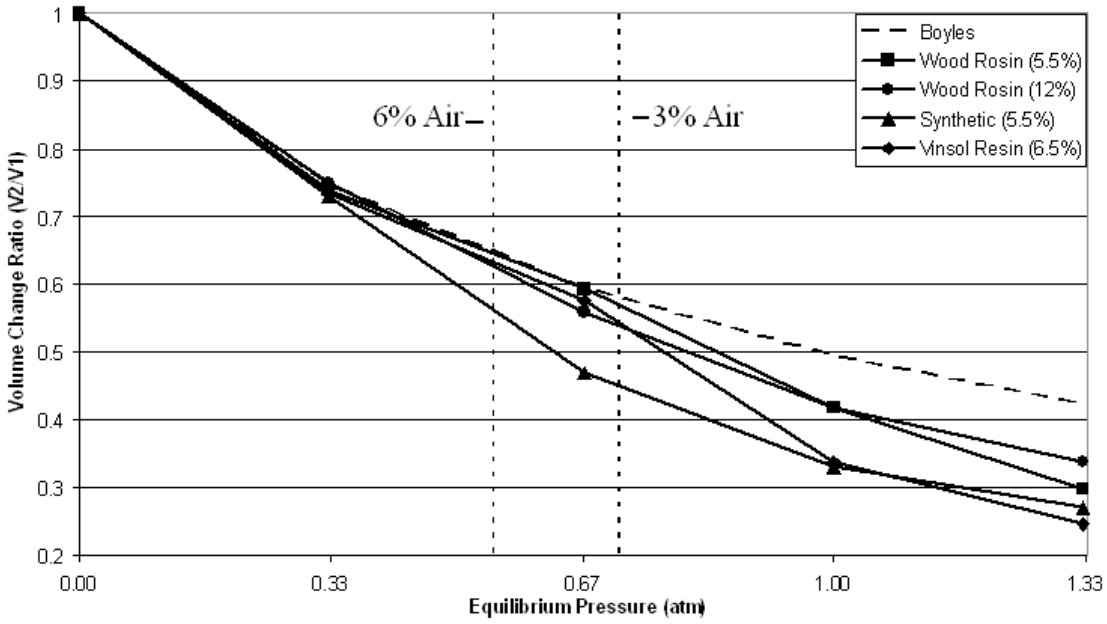

Figure 12: Volume Change Ratios per Pressure Step

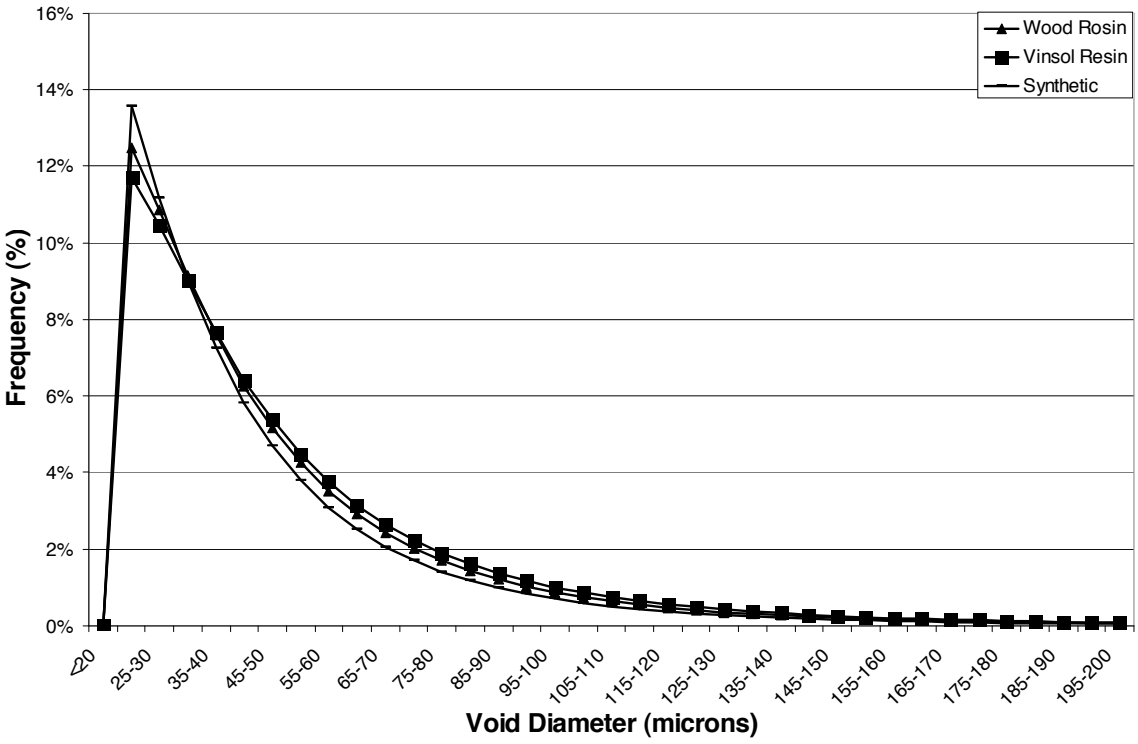

Figure 13: Atmospheric Air-void Distribution Curves

The following graphs display how the 12% air, wood rosin void system changed under pressure. Figure 14(a) shows the measured air-void system, and 14(b) shows how the system would have changed if each void experienced a compression equal to the Boyles law theoretical values provided in Table 4. Figure 15 presents a comparison of Figure 14(a) and (b) for each pressure step. Each graph displays the atmospheric air-void system, the pressurized air-void distribution and its Boyle's Law-only counterpart.

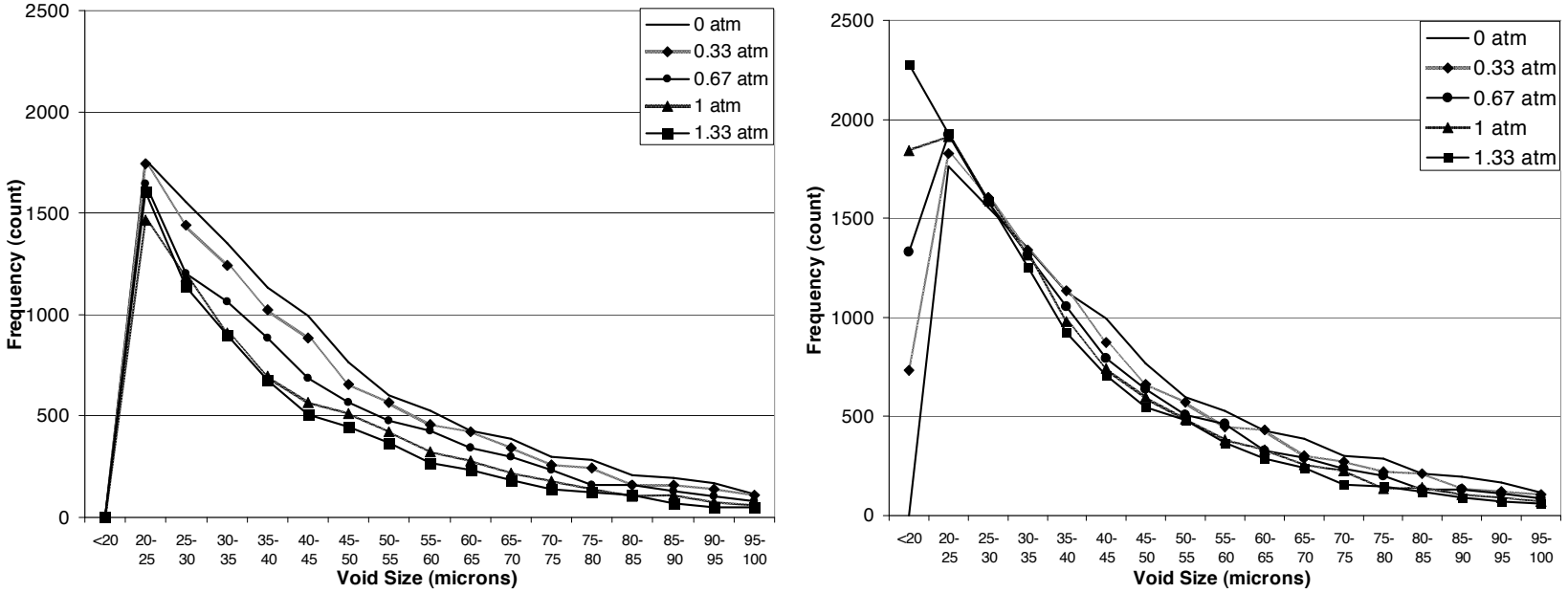

(a) Measured Air Void System Response

(b) Boyle's Law Predicted Void System Response

Figure 14: Air-void Size Distributions Plots – Wood Rosin, 12% Air

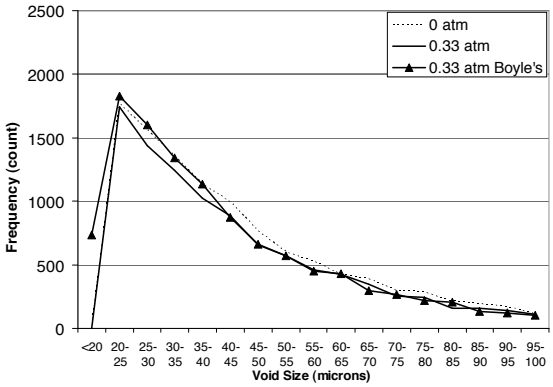

(a) 0.33 atm

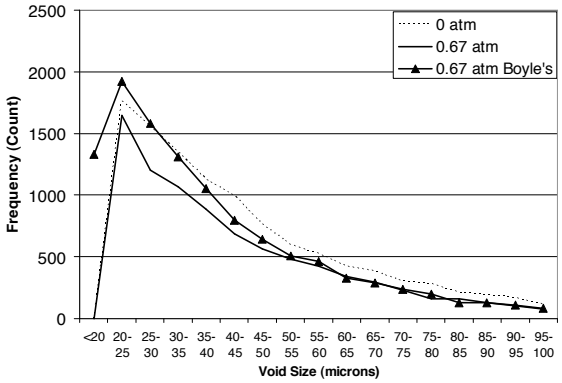

(b) 0.67 atm

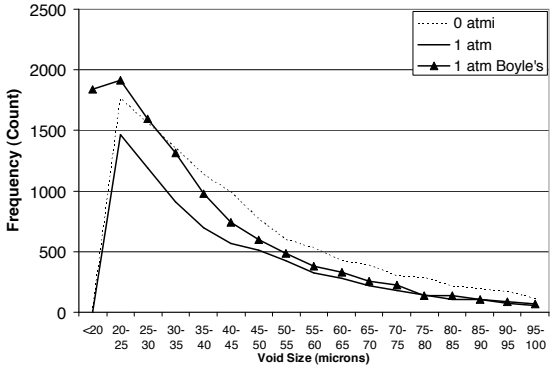

(c) 1 atm

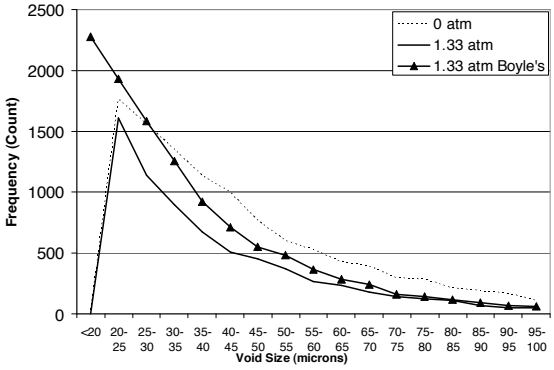

(d) 1.33 atm

Figure 15: Air-void Size Distribution Comparisons – Wood Rosin 12% Air Content

Discussion

Response of Air-void Size to Pressure

From Table 5, it can be seen that the data closely follows the theoretical values suggested by Boyle's Law. Percent differences in the diameter change from values suggested from Boyle's Law range from 0 to 5%. The coefficient of variance for each data set ranges from 5 to 8% with the smallest sample group being 232 measurements. This shows that the data is very accurate and repeatable over a large number of observations. All of these measures are good indicators of the relationship between measured response and Boyle's Law.

The results from these experiments demonstrate that air-voids do not strictly follow Boyle's Law, but have a roughly normal distribution about an average value. This is shown by analyzing the percentage of measurements within one standard deviation of the average. For data sets with a normal distribution, 64% of the data points are within one standard deviation. For the measured data, percentages ranged from 72% to 87%. This suggests that the measured data has a tighter distribution than a normal curve.

Although previous publications have suggested that small air-voids within the entrained air-void system are incompressible[6,9], data for each size range suggests that this is not true for air-voids 49 microns and larger.

Overall this data suggests that Boyle's Law is a good estimate of the over pressure of air-voids that are larger than 49 microns in diameter.

Dissolution of Air-Voids Under Pressure

In Fig. 12 one can see that the volume change of the air void system from a 0.33 atm applied pressure was very similar to the change predicted by Boyle's Law for each AEA investigated. However for the mixture made with the synthetic AEA, significant deviations from Boyle's Law

were observed at all pressures above 0.33 atm. These differences in performance are significant for the pressures typically seen in the ASTM C231 pressure meter. This can be clearly seen as the equilibrium pressure for 6% and 3% has been added to the graph. For pressures larger than the 0.67 atm it can be seen that all of the AEAs start to show a measureable deviation from Boyle's Law with similar values to what is observed in by the synthetic AEAs. It should also be noted that the two different wood rosin mixtures had a very similar performance regardless of the air content in the sample.

As shown in Fig. 12 the air-void size distributions for each air entrainer at atmospheric pressure as measured by the CT scanner is helpful to understand the different behaviors of each AEA investigated. It can be seen that the synthetic AEA has the highest percentage of small voids when compared to the other AEAs. The data in Fig. 12 shows that a synthetic AEA deviated from Boyle's Law the most of the three. One could hypothesize that these small voids are susceptible to dissolving because of their higher internal pressures and that explains the difference in performance of the void systems with pressure. However, the differences observed in the air-void systems at atmospheric pressure for each AEA do not appear significant enough to completely explain the differences observed in Fig. 12. In particular, the large change in volume shown in the Vinsol resin sample between 0.67 and 1 atm based on the size range. If one were to assume that air-void systems with a larger percentage of small voids would demonstrate more volume change due to dissolution, than the wood rosin sample would have demonstrated a similar jump prior to the vinsol resin sample. Thus some other factors are likely contributing. A possible explanation would be that the early age hydration shells around each air-void play a part in the dissolution behavior, and that each air entrainer creates a chemical shell with different properties. These hydration shells have been discussed previously by Ley et al. (2008a, 2008b). In this work it has been shown that there is a significant difference in chemistry, and response to pressure for different AEA hydration shells.

Figures 14 and 15 provide the measured air-void size distributions as well as theoretical distributions for an air-entrained paste sample with wood rosin AEA with12% air by volume. These graphs were chosen as typical examples of the behavior observed. Figure 14(a) shows an overlap of the measured air-void size distribution for each pressure step. Figure 14(b) displays the size distribution predicted by Boyle's Law at each pressure step. One can observe that there is a significant discrepancy in the behavior of the predicted and actual performance. Boyle's Law predicts that the voids that are less than 30 microns should increase in number while the voids larger than 30 microns should decrease in number. The measured data shows that every size range of air-voids are decreasing in number. This data clearly shows that these smaller voids are not increasing in number as is predicted. Instead these voids are likely dissolving into solution as is suggested by Henry's Law.

Figure 15 compares the measured size distribution to the theoretical at each pressure step. In Fig. 15(a) it can be seen that for the 0.33 atm pressure increase that small differences exist between Boyle's Law distribution and the measured system. Although differences exist in ranges up to 40 microns, the total volume dissolved is not significant as seen in Figure 12 at the 0.33 atm data point for this sample. At 0.67 atm, a significant amount of air-voids less than 40 microns dissolve, with few air-voids dissolving above this range. This dissolved volume does register as a measurable deviation from Boyle's Law, but not a significant one as seen in Figure 12. The remaining pressure steps show a great discrepancy in the voids present versus the voids measured at the smaller size ranges. While pressurizing the air-void system the larger voids should shrink in size with the pressure according to Boyle's Law. However the voids at the smaller size range do not show this same change. It appears that the number of voids observed is decreasing in size for the voids smaller than about 50 microns. This difference in the predicted number gets larger with higher pressures. As the pressure is increased the larger voids are getting smaller as predicted by Boyle's Law. However, the smaller voids appear to be dissolving. This is logical as

Henry's Law predicts that gasses will dissolve into solution when pressures are high enough. It appears that this is happening for these smaller bubbles.

These graphs however indicate that as the smallest air-voids are dissolved, they are replaced by the compression of larger air-voids, thus a distribution peak always exists around the 20-25 micron point. It can be observed that if air-voids were not dissolving, this peak would continue to grow as air-voids stacked up in this size range, as shown by the theoretical compression of the system in Figure 14(b).

Interpretation of Results

The errors associated with the pressure meter are not conservative, but instead overestimate the original volume of air. This is because the pressure meter assumes all volume change in the air-void system is due to compression, so the additional volume change due to voids dissolving is interpreted as a higher air content than what actually exists. The exact discrepancy that the measured deviations in volume change would have on the pressure meter is shown in Figure 16. The data from Figure 12 was used to modify the equations for the pressure meter, resulting in new equilibrium pressure – air content curves for each AEA.

From Figure 16 it can be seen that errors upwards of 1% would exist if the synthetic air-entrained mixture behaved similarly in a pressure meter. Even more important is that this error exists in a critical range of air contents. Most specifications require concretes to have 6% air content by volume for freeze-thaw resistance[17]. Figure 16 suggests that a pressure meter would report an air content of 6% when roughly 5% air actually existed within a concrete which utilized a synthetic air entrainer. All other air-entrainer specific curves in Figure 16 show that errors limited 0.25% exist between them and the current pressure meter calibration, with the exception of the vinsol resin curve above 10% air contents.

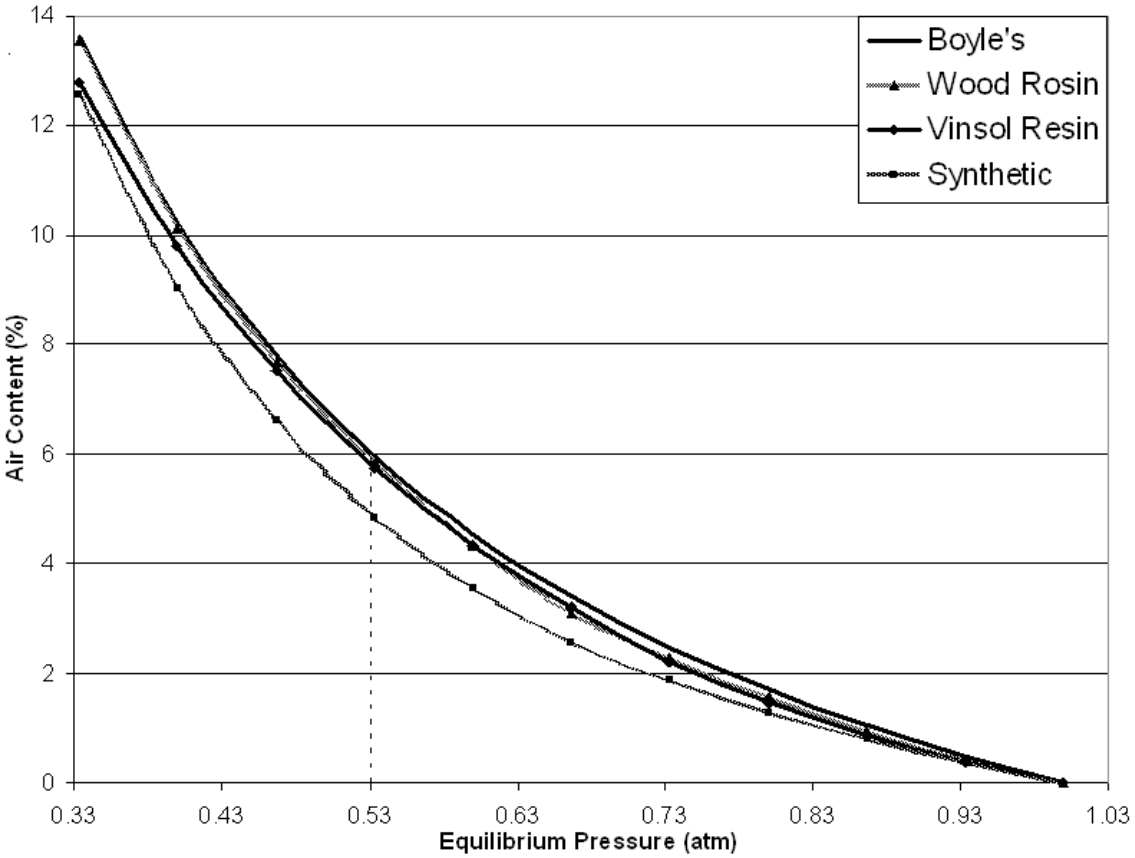

Figure16: Modified Pressure Meter Curve for different AEAs.

Conclusions

This paper has used mCT to investigate the response of air-entrained voids in cement paste to overpressure. This work has shown that air-voids with diameters greater than 50 microns closely follow the prediction of Boyle's Law as the surrounding pressure is increased. In addition it was shown that the void system smaller than 50 microns does not follow Boyle's Law. These voids dissolve with the increase in pressure. This dissolution is not currently taken into account by the current practice with the ASTM C231 pressure meter. Because of this errors can be expected in the measurements. These errors are exasperated with samples that contain high volumes of small voids. In this testing this was observed to occur with synthetic AEAs. The errors estimated can be as high as 1% for synthetic AEAs and about 0.25% for other AEAs. This finding is significant

as this error is likely a contributor to the observed discrepancy between air contents measured in the fresh and hardened state.

In addition this work has shown that 3D void measurements and parameters can be non destructively made for air-void systems in cement paste by using mCT with the procedures outlined in this paper. This is a significant tool that may be able to provide insight into the performance of air-void systems in future research.

CHAPTER III

SUMMARY AND FUTURE WORK

The results of this research suggest that although the Type B pressure meter assumptions are valid for the compression of individual voids, the volume of air-voids which dissolve under pressure is significant enough to register noticeable errors when using a synthetic air-entraining admixture with the Type B pressure meter test. Although further research is needed to add more data points to the graphs shown, results currently suggest that air-void systems with a significant percentage of small voids present will have higher deviation from the Boyle's Law model used by the Type B pressure meter due to the dissolution of these air-voids.

Future work in this area could include repeating experiments to verify results and add additional data points, and using the developed equilibrium pressure-air content graphs to recalibrate the Type B pressure meter. A recalibrated pressure meter could be used in the laboratory on concrete mixtures with results being compared to hardened air-void analysis and additional micro-CT scans.

REFERENCES

[1] Mielenz, R.C., Wolkdorf, V.E., Backstrom, J.E., and Burrows, R.W., "Origin, Evolution, and Effects of the Air Void System in Concrete: Part 4: The Air Void System in Job Concrete," in Proceedings of the American Concrete Institute, Vol. 30, No. 4, 1958, pp. 507-518.

[2] Powers, T.C. "The Air Requirement of Frost-Resistant Concrete," in Proceedings of the Highway Research Board, Vol.29, pp. 184-202.

[3] Hover, K., "Why is There Air in Concrete?" Part 1 of 4, Publication #C930011, Aberdeen group

[4] Scherer, G.W., Valenza II, J.J, "Mechanisms of Frost Damage," Materials Science of Concrete VII, pp.209-245.

[5] Klein, W.H., Walker, S., "A Method for Direct Measurement of Entrained Air in Concrete," Journal, American Concrete Institute, Vol. 42, p.657

[6] Hover, K., "Analytical Investigation of the Influence of Air Bubble Size on the Determination of the Air Content of Freshly Mixed Concrete," Cement, Concrete and Aggregates, CCAGDP, Vol.10, No. 1, Summer 1988, pp.29-34.

[7] Gay, F. T., "The Influence of Thermal History on Air Content and Air-Void System Parameters of Concrete of Differing Cement Factors." Proceedings of the Sixth International Conference on Cement Microscopy, Page 384, 1984.

[8] Gay, F. T., "The Effect of Mix Temperature on Air Content and Spacing Factors of Hardened Concrete Mixes with Standardized Additions of Air-Entraining Agent." Proceedings of the Seventh International Conference on Cement Microscopy, Page 305, 1985

[9] Gay, F. T., "A Factor Which May Affect Differences in the Determined Air Content of Plastic and Hardened Air-Entrained Concrete." Proceedings of the Fourth International Conference on Cement Microscopy, Page 276, 1982

[10] Hover, K., "Some Recent Problems with Air-Entrained Concrete," Cement, Concrete and Aggregates, CCAGDP, Vol.11, No. 1, Summer 1989, pp.67-72.

[11] Whiting, D. and Stark, D., "Control of Air Content in Concrete," National Cooperative Highway Research Program Report 258, Transportation Research Board, National Research Council, Washington, DC, May 1983

[12] Ozyildirim, C., "Comparison of the Air Contents of Freshly Mixed and Hardened Concretes," Cement, Concrete, and Aggregates, CCAGDP, Vol. 13, No. 1, Summer 1991, pp. 11-17

[13] Elkey, W.D., Jansen, D.J., and Hover, K.C. "Effects of Admixtures on Air-Void Stability of Concrete Subjected to Pressurization," CONSEC '98, International Conference on Concrete Under Severe Conditions, Tromso, Norway, 1998.

[14] Stock, S.R., "MicroComputed Tomography: Methodology and Applications," Boca Raton, CRC Press, 2008.

[15] Natterer, F., Wubbeling, F., "Mathematical Methods in Image Reconstruction," Vol. 5 of SIAM Monographs on Mathematical Modeling and Computation, Cambridge University press, 2001.

[16] Hsieh, J. "Computed Tomography: Principles, Design, Artifacts and Recent Advances," Vol. 114 of Progress in Biomedical Optics and Imaging, SPIE Press, 2003

[17] Kosmatka, S., Kerkhoff, B., and Panarese, W. "PCA Design and Control of Concrete Mixtures," Portland Cement Association, 2008.

VITA

Robert Frazier

Candidate for the Degree of

Master of Science

Thesis: RESPONSE OF ENTRAINED AIR-VOID SYSTEMS IN CEMENT PASTE TO PRESSURE

Major Field: Civil Engineering

Biographical:

Education:

Completed the requirements for the Master of Science in Civil Engineering at Oklahoma State University, Stillwater, Oklahoma in July, 2011.

Completed the requirements for the Bachelor of Science in Civil Engineering at Oklahoma State University, Stillwater, Oklahoma in 2008.

Name: Robert Frazier Date of Degree: July, 2011

Institution: Oklahoma State University Location: Stillwater, Oklahoma

Title of Study: RESPONSE OF ENTRAINED AIR-VOID SYSTEMS IN CEMENT PASTE TO PRESSURE

Pages in Study: 38 Candidate for the Degree of Master of Science

Major Field: Civil Engineering

Scope and Method of Study:

Determine the response of entrained air-void systems in fresh cement paste to applied pressures by utilizing micro-computed tomography. Compare results to those suggested by the ASTM C231 Type B pressure meter calibration equations.

Findings and Conclusions:

The results of this research suggest that although the Type B pressure meter assumptions are valid for the compression of individual voids, the volume of air-voids which dissolve under pressure is significant enough to register noticeable errors when using a synthetic air-entraining admixture with the Type B pressure meter test. Results currently suggest that air-void systems with a significant percentage of small voids present will have higher deviation from the Boyle's Law model used by the Type B pressure meter due to the dissolution of these air-voids.

ADVISER'S APPROVAL: Dr. Tyler Ley